A second cochlear-frequency map that correlates distortion product and neural tuning measurements

J. B. Allen
Acoustics Research Department, AT&T Bell Laboratories, Murray Hill, New Jersey 07974

P. F. Fahey
Department of Physics, University of Scranton, Scranton, Pennsylvania 18510

(Received 8 October 1992; accepted for publication 19 March 1993)

Acoustic intermodulation distortion products (DPs) are generated by the nonlinear motion of the basilar membrane (BM) in the cochlea, and propagate back to the ear canal where they may be measured. One common method of measuring these distortion products is to hold the higher-primary frequency f_2 fixed while varying the lower-primary frequency f_1. When doing this, it is well known that the ear canal distortion product is maximum for a particular value of f_2/f_1, usually between 1.1 and 1.4. In fact *all* odd order distortion products of the form $f_d^{(n)}=f_1-n(f_2-f_1)$, $n=1,2,3,...$ are maximum at the same $f_d^{(n)}$, independent of the order n, but dependent on f_2 which determines the place of DP generation. In this paper, it is argued that this maximum must result from filtering by micromechanical resonances within the cochlea. In fact the frequency where the neural tuning curve "tip" meets the "tail" is the same as the frequency where the distortion products are maximum. This suggests that each section of the basilar membrane must consist of two resonant impedances. The first is the usual series basilar membrane resonant impedance that gives rise to the characteristic frequency (CF). The second resonant impedance must be tuned to a frequency that is lower than the CF and must act as a shunt across the inner hair-cells, since it acts to *reduce* the forward transmission to the neuron, while, at the same time, it maximally couples all the distortion products back into the cochlear fluids, giving them a frequency dependent *increase* at its resonant frequency. Thus the proposed second mechanical resonance concept explains a great deal of complicated and confusing data. For pure tone excitation, the second resonance modifies the traveling wave excitation pattern (EP) basal to its characteristic place (CP). A good candidate for this second mechanical resonance would be a resonance of the tectorial membrane (TM), tuned to the neural tip-tail frequency at each place.

PACS numbers: 43.64.Bt, 43.64.Jb, 43.64.Kc, 43.64.Pg

INTRODUCTION

Nonlinear acoustic distortion products of odd-order are known to be generated on the basilar membrane (BM) in response to two primary tones, at frequencies f_1 and f_2, with $f_2>f_1$, and at pressure levels P_1 and P_2. After being generated, these distortion products propagate back along the basilar membrane to the ear canal, where they may be measured with a microphone. The frequency of the distortion product f_d may be independently varied, for a fixed f_2, by varying f_1 and by choosing the DP *order n*. We shall look at the distortion products that are just below f_1 in frequency, namely $f_d^{(n)}=f_1-n(f_2-f_1)$. For $n=1$, $f_d=2f_1-f_2$. It has been shown in guinea pig and human (Brown and Gaskill, 1990; Brown *et al.*, 1992), cat (Fahey and Allen, 1986), and rabbit (Whitehead *et al.*, 1992), that the first order ($n=1$) distortion product $2f_1-f_2$ is maximum when f_2/f_1 is approximately 1.1 to 1.4. It is *not* as well known that when f_2 is held fixed, all the DPs are maximum at the same frequency, independent of the order n (Fahey and Allen, 1986, page 320, Fig. 5; Brown and Gaskill, 1990; Brown *et al.*, 1992).

In this paper we study the question, *Why do the ear canal distortion products rise to a maximum and then decrease as f_1 approaches f_2?* There are two obvious possible explanations of this phenomenon, *suppression* and *filtering*. The suppression hypothesis argues that one primary suppresses the other as the primary frequencies come together, decreasing the distortion product level. The filtering hypothesis argues that the distortion product is filtered by the micromechanics of the organ of Corti, by a filter tuned to the maximum DP frequency, which is determined by the DP generation site.

We may choose between these two possibilities by looking at the frequency response of the distortion product as a function of the DP order n. Since the DPs are maximum at the same frequency, independent of their order, and, thereby, necessarily independent of f_1, we conclude that they have been *filtered* by the micromechanics rather than having been suppressed. This raises the interesting possibility that neural tuning might be correlated to distortion product tuning.

In this paper we describe such a correlation. Namely we show a correlation between the frequency where the distortion products are maximum and the frequency where the tip and the tail join on the neural tuning curve recorded from the f_2 place, for 2 kHz$\leqslant f_2$ 20 kHz. We then show that this correlation can be explained by a mechanical resonance tuned to a frequency below the resonant frequency

 0001-4966/93/94(2)/809/8/$6.00

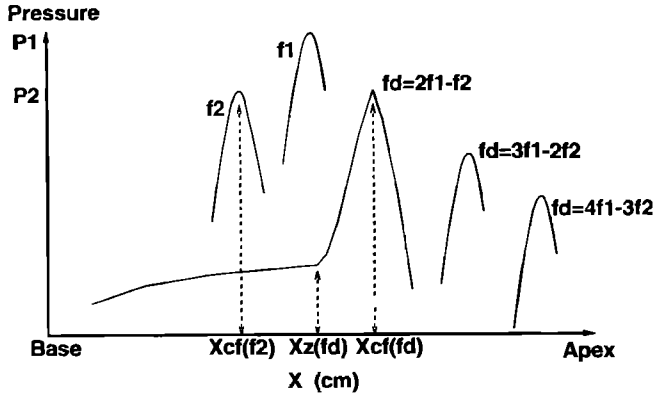

FIG. 1. The partial excitation patterns are shown for the conditions of the distortion product generation. Since f_2 is higher in frequency than f_1, its excitation pattern is basal to that of f_1. The DP $2f_1 - f_2$, being lower in frequency than both f_1 and f_2, is apical to both. It is also lower in level on the basilar membrane by about 40 dB.

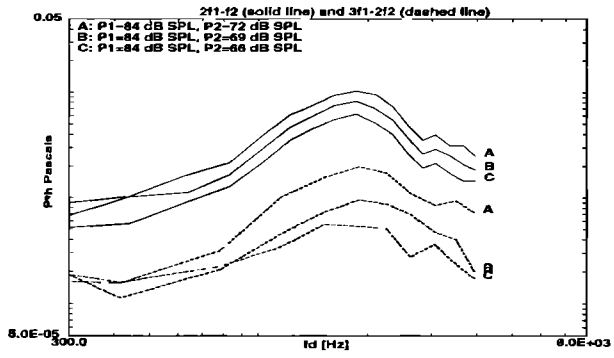

FIG. 2. Cat distortion products $2f_1 - f_2$ (solid line) and $3f_1 - 2f_2$ (dashed line) for a fixed f_2 of 4 kHz. The primary levels were $P_1 = 84$ and $P_2 = 72$, 69, 66 dB SPL. The maximum DP level at f_d^* is just below 2.0 kHz for this example.

(CF) of the basilar membrane. This second tuned impedance must appear as a velocity-shunt to the cilia motion to account for the correlation between the frequency responses of the distortion products and the neural tuning curves.

I. DISTORTION PRODUCT GENERATION

First we describe distortion product generation and the data that leads us to the conclusion that the distortion products are tuned.

Figure 1 is a cartoon depicting the tips of the excitation patterns for f_2 and f_1, along with the excitation pattern for the $f_d^{(n)} = f_1 - n(f_2 - f_1)$ $(n = 1,2,3,\ldots)$ DP. The greater the distortion product order n, the lower the DP frequency and the further its excitation pattern shifts to the right. In the figure we label the various features seen in the excitation pattern. We define the *characteristic place* (CP) $x_{CF}(f)$ as the location on the basilar membrane where the excitation pattern is maximum, for a given input tone having frequency f. The CP for f_2 is $x_{CF}(f_2)$, while $x_{CF}(f_d)$ is the CP for the distortion product.

To generate a distortion product on the basilar membrane, two primary tones having pressure P_1 and P_2 are presented to the ear canal, giving rise to the two excitation patterns (EPs) shown in Fig. 1 that peak at $x_{CF}(f_2)$ and $x_{CF}(f_1)$. We shall look at intermodulation distortion products generated by the nonlinear basilar membrane interactions of the primaries at frequencies $f_1 - n(f_2 - f_1)$, where n is any integer. With $n > 1$, the distortion products have frequencies lower than either of the primaries, while for $n \leqslant -2$, the distortion product frequencies are higher than either primary. The most interesting of these, and the ones that we will describe here, are the first three lower frequency distortion products $(n = 1,2,3)$.

The distortion product is generated in a region along the basilar membrane corresponding to the maximum overlap of the two primary excitation patterns. This place is believed to be near, or at, the f_2 place (Matthews and Molnar, 1986). At low frequencies, say below 1 kHz, where the high frequency slope is not as sharp, the source location could spread toward the f_1 place. We are not aware of any data that confirms this possibility however.

The nonlinear component of the motion at the generator site is believed to be the source of the distortion products. Any source on the basilar membrane generates waves which propagate both to their corresponding characteristic place $x_{CF}(f_d)$, and back to the ear canal (Hall, 1974; Kim *et al.*, 1979; Fahey and Allen, 1985).

A. Relation between maximum DP and f_2

Frequency $f_d^*(f_2)$ is defined as the frequency corresponding to the maximum distortion product. Assuming $f_2 \geqslant 2$ kHz, with fixed f_2, f_1 varied, and $n > 1$, the distortion product pressure $P(f_d)$ is maximum at frequency $f_d^*(f_2)$, *dependent* on f_2 and *independent* of f_1 and n (Brown and Gaskill, 1990; Fahey and Allen, 1986; Fahey and Allen, 1988). In other words, each distortion product, $2f_1 - f_2$, $3f_1 - 2f_2$, and $4f_1 - 3f_2$, has a *maximum pressure at the same frequency.* It follows that they must be maximum for different f_2/f_1 ratios.

In Fig. 2 we show DP data for $n = 1$ and $n = 2$ for a fixed f_2 of 4 kHz for the cat. In this case the DP shows a maximum at a frequency slightly below 2 kHz.

In Fig. 3 we show the $n = 1$ DP in a human ear for primary levels of 65 dB SPL, for six different f_2 values. In one case, for f_2 near 2 kHz, the DP response has a "notch," leading to a non-monotonic response. These notches are strongly dependent on the primary signal levels. By taking data at slightly different levels of P_2, the notches may be avoided.

In Fig. 4 we see DP data for $n = 1,2$ for the cat. Since this data was taken at very high sound pressure levels, the curves appear less regular than the data of Fig. 4. However we see that each response is tuned in a manner that depends on f_2.

Brown and Gaskell (1990) have presented similar data in several other species, and have observed similar relations between the higher-order distortion products.

We, and Brown and Gaskill (1990), independently draw the following conclusions: (a) because $f_d^*(f_2)$ is independent of n, the distortion products must be filtered by a band-pass filter tuned to $f_d^*(f_2)$, (b) because $f_d^*(f_2)$ is

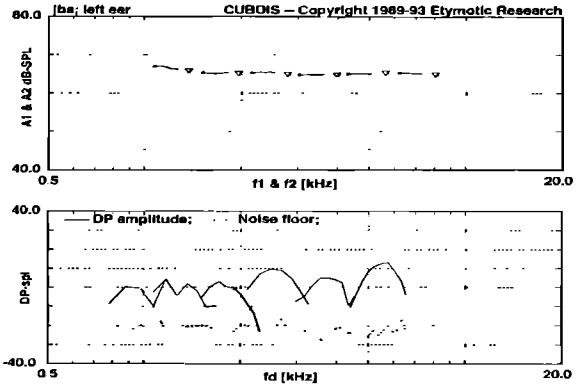

FIG. 3. The upper panel shows the primary levels used to measure the distortion products $2f_1 - f_2$ in the human ear as a function of f_2 using the CUBDIS™ measurement system (Etymotic Research, Elk Grove Village, IL). In the upper panel the primary levels are shown. The triangle gives the frequency and level of P_2, while the solid line shows the swept frequencies and levels of P_1. In the lower panel the corresponding $2f_1-f_2$ level (solid line) is shown, plotted as a function of $f_d=2f_1-f_2$. The dashed lines show the noise floor corresponding to the DP measurement.

independent of f_1, this filter must be associated with the place of DP generation, namely x_2.

B. Relation of f_d^* to f_2

In Fig. 5 we show the $f_d^*(f_2)$ data points for the cat. We have taken data from earlier work (Fahey and Allen, 1986) and from unpublished data. The x's represent the $2f_1-f_2$ data and the o's represent the $3f_1-2f_2$ data. The dashed line is given by

$$f_d^*(f_2)=0.08f_2^{1.22}. \quad (1)$$

Similar data for human subjects, such as the data of Fig. 3, give a different relation for $f_d^*(f_2)$, namely $f_d^*(f_2)=0.5f_2^{1.04}$. Thus $f_d^*(f_2)$ for cat and human are different.

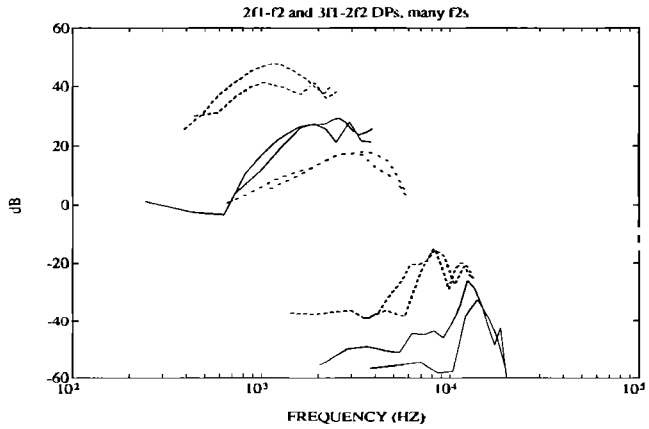

FIG. 4. Distortion products $2f_1 - f_2$ and $3f_1 - 2f_2$ for six different f_2 values for the cat (f_2=2.6, 4.0, 5.9, 8.9, 13.3, and 20 kHz). The $3f_1 - 2f_2$ DP's have been shifted up by 5 dB. Each pair of curves has been displaced by 20 dB for clarity. The primary levels were approximately 96 dB SPL for this figure. At these high levels many "notches" begin to appear. However the DP levels still decrease as f_1 approaches f_2 for both types of DP's.

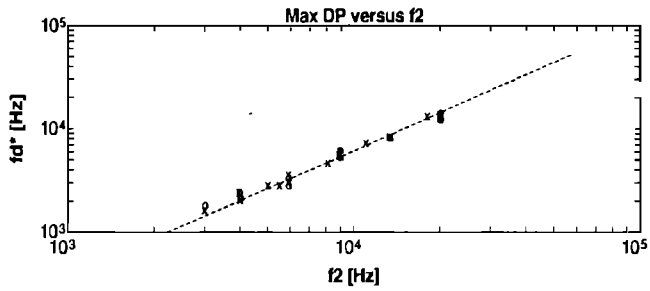

FIG. 5. The x's show the frequencies $f_d^*(f_2)$ corresponding to the maximum DP for $2f_1-f_2$ while the o's show them for $3f_1-2f_2$. The dashed line is given by $f_d^*=0.08f_2^{1.22}$, Eq. (1).

For $f_2 \geqslant 2$ kHz, the distortion products that have higher frequencies than the primaries, such as $2f_2-f_1$ ($n=-2$) and $3f_2-2f_1$ ($n=-3$), do not show these maxima (Fahey and Allen, 1988 and unpublished data). Generally these higher frequency distortion products approach their maximum when frequencies f_2 and f_1 are almost equal (at maximum overlap of the f_2 and f_1 excitation).

II. NEURAL FREQUENCY TUNING CURVES

As mentioned in the Introduction, we will describe a correlation between cochlear tuning, as measured by neural tuning curves, and DP tuning. In order to understand this relationship several definitions are necessary.

A. Definition of terms

The *neural frequency tuning curve* (FTC) is defined as the ear canal pressure $P_0(f, x_0)$ at a defined threshold criterion (usually one neural spike per 50 millisecond interval above spontaneous) for excitation of a neuron innervating location x_0 on the basilar membrane, as a function of frequency f. Figure 6 shows a family of such FTC's as measured in the cat. The most sensitive frequency f_{CF} is called the *characteristic frequency*, or CF. The CF of the neuron tuned to 6 kHz in Fig. 6 is labeled Fcf.

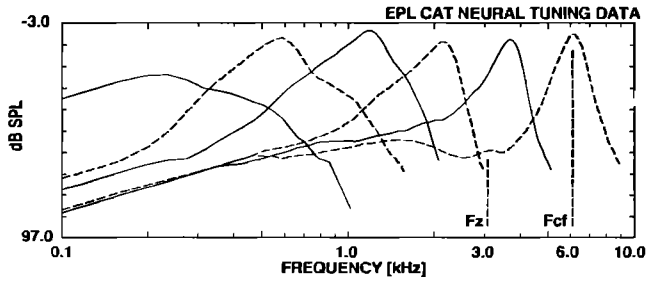

FIG. 6. Shown here are a family of cat frequency tuning curves, defined as the ear canal pressure that will just excite the neuron (note that the amplitude scale is inverted). Each curve corresponds to a single neuron. The location of the neuron may be determined from the cochlear map function. The 6-kHz CF is indicated by Fcf. The frequency where the tip and tail meet for the 6-kHz CF neuron is indicated by Fz and is 3 kHz. The data used to construct these curves were provided by M.C. Liberman and B. Delgutte of the Mass Eye and Ear Infirmary, Boston, MA.

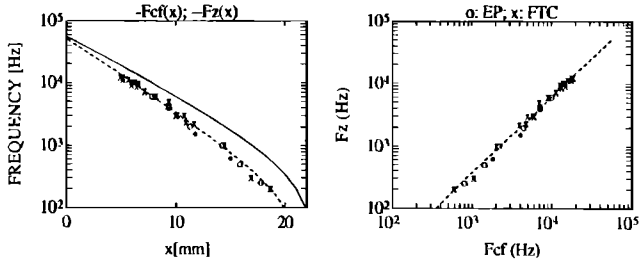

FIG. 7. **Left:** The upper solid curve is a plot of $f_{CF}(x)$ for the cat as a function of position along the basilar membrane. The dashed curve shows $f_z(x)$. The o's are inflection points taken from the excitation patterns. The x's are points taken from the frequency tuning curves where the tip meets the tail (data from 12 animals). The *'s are taken from Kim *et al.* (1979). **Right:** In this panel we have plotted $f_z(x)$ as a function of $f_{CF}(x)$ for each x value. The data points fall on a straight line on a log-log frequency plot. The equation for the dashed lines is given by $f_z = 0.08 f_{CF}^{1.22}$, Eq. (2).

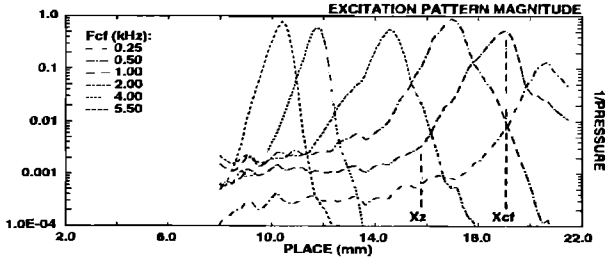

FIG. 8. This family of neural excitation patterns has been derived from a large number of FTC's, including those of Fig. 6, using the cochlear map function shown in Fig. 5 (solid) left. Feature x_z at 15 mm for the EP corresponding to 500 Hz (x_{CF}=19 mm) is labeled. It is determined by the place where the slope of the EP sharply changes. The EP for each frequency shows such a slope change. The points of these inflection points are plotted in Fig. 7 (Left) as circles. The data used to construct these curves was provided by M.C. Liberman and B. Delgutte of the Mass Eye and Ear Infirmary, Boston, MA.

1. The cochlear frequency map

The *cochlear frequency map* is defined as the functional relationship of the CF as a function of place x along the basilar membrane. The cochlear map function is shown in Fig. 7 (Left) as the solid curve, and is known from experiments. The cochlear map function $f_{CF}(x)$, which describes the characteristic frequency as a function of place, was determined by Liberman (1982) for the cat using chemical markers following neural tuning curve measurements. Since the cochlear map is a single valued function, its inverse $x_{CF}(f)$, which describes the characteristic place as a function of frequency, is also known.

B. Neural excitation patterns

The *excitation pattern* (EP) is defined as the response along the basilar membrane to a pure tone. However, it is very difficult, if not impossible, to obtain the EP directly because it requires the simultaneous measurement of many points along the basilar membrane. A function closely related to the EP may be derived from a family of neural tuning curves in a straight forward manner. Each neural tuning curve $P_0(f,x_0)$ represents the threshold pressure as a function of frequency f corresponding to a hair-cell located at x_0 on the basilar membrane. At one frequency, f_{CF}, the pressure is minimum, indicating the most sensitive frequency of the neuron. From the cochlear map (see Fig. 7), x_0 may be determined once f_{CF} is known since $x_0 = x_{CF}(f_{CF})$. Given many such tuning curves, and given the cochlear map function, one may convert the neural tuning curves into functions of x for a fixed frequency. These derived functions $P_0(f_0,x)$, plotted as a function of x for a given frequency f_0, will be called *neural excitation patterns*. Instead of plotting the pressure, we plot the reciprocal pressure, giving a display that is similar to the cilia (hair cell shear) stimulus. Because of the basilar membrane nonlinearity, the derived neural excitation pattern is not the same as the cilia excitation pattern for a fixed input level. One may consider the neural excitation pattern as a plot of the reciprocal pressure required to excite each neuron at threshold. Further detail for constructing the neural excitation patterns is given in Allen (1990).

In Fig. 8 a family of neural excitation patterns, derived from the FTC's of Fig. 6, are shown. The characteristic place $x_{CF}(f)$ is the location on the basilar membrane where the excitation pattern is maximum, for a given input tone having frequency f. The CP for the 500-Hz tone is labeled as Xcf and is approximately 19 mm.

1. A second cochlear map

When looking at families of FTC's, a second cochlear map, which we call $f_z(x)$, may be defined. Function $f_z(x)$ describes the frequency of the tuning curve where the *tip* and *tail* join. In Fig. 6 the frequency f_z at 3.0 kHz is labeled for the 6-kHz FTC. This feature, although present, is not clearly seen at the lower frequencies because it is obscured by the many other sub-systems that also depend on frequency, such as the middle ear and the hair-cells. When viewing excitation patterns however, each frequency response is constant, since tones having a single frequency are used as the input. In this case the junction between tip and tail becomes well delineated at all frequencies, as may be seen from Fig. 8 where $x_z(f)$ labels the change in EP slope. The functions $x_z(f)$ and $f_z(x)$ are inverses of each other, as is the case for the cochlear frequency map $x_{CF}(f)$ and $f_{CF}(x)$. For example, in Fig. 8 we show x_z at 16 mm for the 500-Hz EP having its x_{CF} at 19 mm. The x_z for a 1-kHz tone is near 14.1 mm, and for a 2-kHz tone x_z is approximately 11.3 mm.

The function $f_z(x)$ is shown in Fig. 7 (Left) as the dashed curve. The o's on that curve represent data taken from the neural excitation patterns, while the x's are data points taken from frequency tuning curves. At low frequencies the EP's define $x_z(f)$ most clearly. At high frequencies f_z may be directly estimated from the FTC. However the effect of f_z may be seen in the FTC's at low frequencies. For example, the slope inflection at 16 mm for the 500-Hz EP (Fig. 8) shows up at 200 Hz on the FTC tuned to 590 Hz.

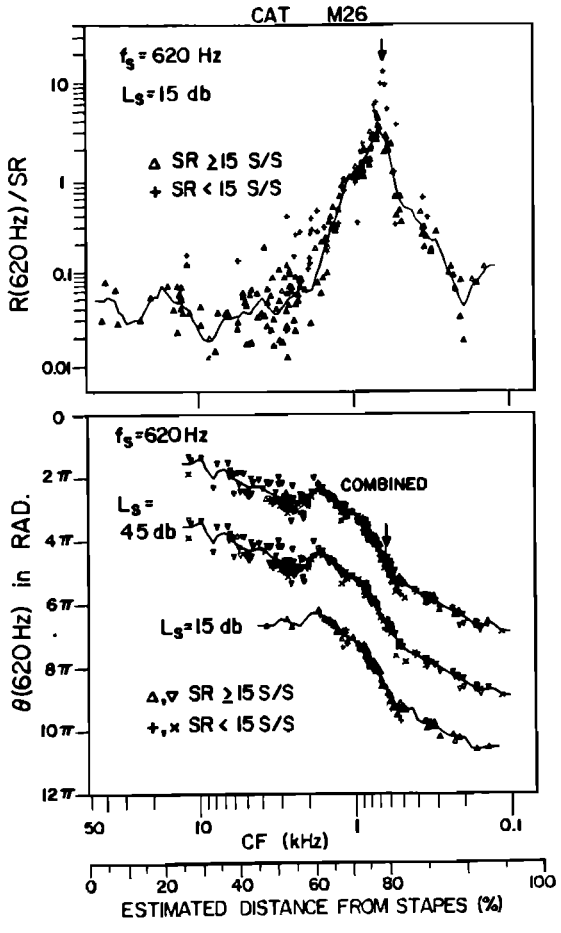

FIG. 9. Figure from Kim *et al.* (1979) which shows the rate and phase of a 620 Hz tone at 15 and 45 dB SPL for hundreds of neurons, plotted as a function of each neuron's characteristic frequency. As before, we define $x_z(f_0)$ as the place where the excitation pattern changes its slope. This place depends on the tone frequency f_0= 620. In their study they used two tone frequencies, f_0 of 620 and 1550 Hz. Note how the neural phase jumps by 180 degrees at x_z.

To determine the frequency of f_z for a given f_{CF} from Fig. 7 (Left), one must use the same abscissa, since a tuning curve is measured for a neuron at one place. When determining x_z corresponding to a given x_{CF} from Fig. 7 (Left), one must use the same ordinate, since in that case the frequency is fixed. The curve $f_z(x)$ was first described in Allen (1980).

2. A third measure of $f_d^*(f_2)$

Kim *et al.* (1979) and Kim *et al.* (1980) measured the response of many neurons to small number of tones, and plotted the rate and the phase as a function of the neurons characteristic frequency. This gave a neural excitation pattern corresponding to a fixed tone. We reproduce some of their data in Fig. 9 , which shows the neural rate and the phase for a 620 Hz tone at two levels, 15 and 45 dB SPL. In the neural excitation patterns of Figs. 1 and 8, the tones are not fixed in level, while in Fig. 9 only one tone level is used for each curve. We may estimate $x_z(f_0)$ from the Kim data from f_0=620 Hz and $f_{CF}(x_z)$ = 1800 Hz. They repeated the experiment with f_0=1550 Hz where they found $f_{CF}(x_z)$ = 4000 Hz. These two data points are shown as the *'s in Fig. 7.

The phase properties of the neural excitation pattern are of significant interest because at $x_z(f_0)$ the phase jumps by 180 degrees (π radians). This phase behavior is a clear indication of a two-component cancellation taking place at x_z. The Kim *et al.* studies used two different frequencies. They found that the phase jump depended on the tone frequency which was at x_z in both cases. *We conclude that the phase jump they found for these two tones is a general property of $x_z(f)$ at all frequencies.*

C. The relation of f_z to f_{CF}

When plotting $\log(f_z)$ against $\log(f_{CF})$, we have found that the data points fall on a straight line, as shown in Fig. 7 (Right, dashed line). The dashed line in this figure is given by

$$f_z = 0.08 f_{CF}^{1.22}. \tag{2}$$

The formula for $f_{CF}(x)$ as given by Liberman (1982) is

$$f_{CF}(x) = 456(10^{2.1(1-x/L)} - 0.8). \tag{3}$$

Substitution of Eq. (3) into Eq. (2) defines the relation $f_z(x)$ shown in Fig. 7 (Left). Liberman estimated a cochlear length of L=2.5 cm for the cat cochlea rather than the 2.2 cm assumed in this paper (Greenwood, 1990). This difference in assumed basilar membrane length has no effect on the conclusions of this paper.

D. What is the meaning of $f_z(x)$?

We shall show that the frequency defined by this second cochlear map plays an important role in both cochlear tuning and in distortion product response. We will argue that the feature labeled by x_z and f_z is due to a second resonance within the organ of Corti (e.g., in the micromechanics).

III. COMPARISON OF $f_d^*(f_2)$ AND $f_z(f_2)$

The two sets of relations, Eq. (1) (determined from DP data), and Eq. (2) (determined from FTC data), describe the same function.

What is the meaning of Eqs. (1) and (2) being the same function? It means that *the distortion product is maximum when its frequency is equal to the tip-tail frequency $f_z(f_2)$ corresponding to the higher frequency primary's place x_2.* In terms of equations, this condition is

$$f_d^*(f_2) = f_z(f_2). \tag{4}$$

Next we explain why this must be true.

When we fix f_2, we fix the generator site at x_2 = $x_{CF}(f_2)$. Referring to Fig. 7 (Right) and Eq. (2), we determine f_z at x_2 to be

$$f_z(f_2) = 0.08 f_2^{1.22}. \tag{5}$$

By substitution of Eq. (5) into Eq. (1) we find the condition of the maximum distortion product Eq. (4).

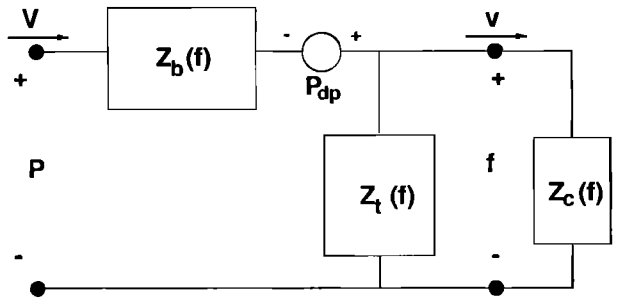

FIG. 10. Block diagram showing the type of impedance relationships that must exist within the organ of Corti to account for the observed relation between the FTC's and the ear canal DPs. The distortion product source is shown as P_{dp}.

We may alternatively think in terms of the excitation patterns shown in Fig. 1. When $f_d = f_d^*$, where is $x_z(f_d)$ relative to $x_2 = x_{CF}(f_2)$? *The distortion product is maximum when the place of the slope-inflection in the neural excitation pattern for the distortion product $x_z(f_d)$ is at the higher frequency place x_2.* In terms of equations, this condition is

$$x_{CF}(f_2) = x_z(f_d^*). \tag{6}$$

To see this we must use Fig. 7 (Left) and a graphical construction. In the figure, pick an x_2 and draw a vertical line. This line crosses the dashed curve at $f_z(f_2)$ and the solid line at f_2. From Eq. (4), this value of $f_z(f_2)$ is also the frequency of the maximum distortion product. Thus if we draw a horizontal line at frequency $f_z(f_2)$ then it crosses the solid line at the maximum DP's characteristic place $x_{CF}(f_d^*)$ (see Fig. 1). To find $x_z(f_d^*)$, move back along the horizontal line to the dashed line, which is the same as $x_{CF}(f_2)$, confirming Eq. (6).

Next we discuss the correspondence between Eqs. (1) and (2) in terms of the physics of the organ of Corti.

IV. THE MICROMECHANICS OF THE SECOND RESONANCE

To describe our results physically we introduce the concept of a linear *two-port* model to relate the basilar membrane velocity $V(f,x)$ and pressure $P(f,x)$ to the outer hair cell (OHC) cilia velocity $\mathrm{v}(f,x)$ and force $\mathrm{f}(f,x)$ (Allen and Neely, 1992). We choose this formulation because it makes no assumptions about the relation between the basilar membrane and the hair cells other than linearity. In terms of the 2×2 matrix of frequency and place dependent components $A(f,x)$, $B(f,x)$, $C(f,x)$, $D(f,x)$,

$$\begin{bmatrix} P(f,x) \\ V(f,x) \end{bmatrix} = \begin{pmatrix} A(f,x) & B(f,x) \\ C(f,x) & D(f,x) \end{pmatrix} \begin{bmatrix} \mathrm{f}(f,x) \\ \mathrm{v}(f,x) \end{bmatrix}. \tag{7}$$

As shown in Fig. 10 we assume that at each point x along the organ of Corti three impedances are defined: Z_b, Z_t, and Z_c. The outer hair cell cilia impedance is the output load, and is defined as $Z_c = \mathrm{f}/\mathrm{v}$. This impedance is assumed to be the cilia stiffness in series with a resistor that represents the damping of the fluid space between the tectorial membrane and the reticular lamina (Allen, 1980). The impedance Z_b is in series with the input, while Z_t shunts the output. These latter two impedances are assumed to have mass components, giving them a resonant frequency. We define the resonant frequency of Z_t as f_z.

Since $|Z_t|$ is minimum at its resonant frequency f_z, if $|Z_t| < |Z_c|$ at f_z, then the neural tuning curve will be less sensitive at f_z because some velocity will be shunted through Z_t. This impedance can also maximally couple the distortion products back into the basilar membrane and cochlear fluids at f_z, as observed.

In terms of Fig. 10, A, B, C, and D are (Allen and Neely, 1992; Allen, 1980)

$$A = 1 + Z_b/Z_t \tag{8}$$

$$B = Z_b \tag{9}$$

$$C = 1/Z_t \tag{10}$$

$$D = 1. \tag{11}$$

The transfer function $H_0 = \mathrm{v}/V$ is

$$H_0(x,f) = \frac{1}{CZ_c + D} \tag{12}$$

$$= \frac{1}{Z_c/Z_t + 1}, \tag{13}$$

while the partition (basilar membrane) impedance $Z_p(x,f) = P/V$ is given by

$$Z_p(x,f) = \frac{AZ_c + B}{C + DZ_c} \tag{14}$$

$$= \frac{(1 + Z_b/Z_t)Z_c + Z_b}{Z_c/Z_t + 1} \tag{15}$$

$$= H_0[(1 + Z_b/Z_t)Z_c + Z_b]. \tag{16}$$

The observation that f_z (the frequency where the tip joins the tail of the neural tuning curve) and f_d^* (the frequency of maximum DP) are at the same frequency is explained by assuming that both Eqs. (13) and (16) are dominated by the impedance of Z_t at its resonance frequency f_z. This condition requires that Z_t shunt the cilia velocity v away from the output impedance Z_c at f_z, and back into the cochlear fluids, namely that $|Z_t| < |Z_c|$. It is also necessary that $|Z_b|$ not be large relative to $|Z_t|$. A proper study of these conditions requires an analysis of the poles and zeros of H_0 and Z_p.

A. Location of the nonlinear element

We now argue that the nonlinear element that generates the distortion products must be in the basilar membrane stiffness. Many models have taken it to be in the resistance component in cochlear amplifier models. We shall show that this is unlikely, based on the impedance of the basilar membrane at the generator site.

In Fig. 11 we show the neural excitation patterns for the two primary signals at frequencies f_1 and f_2, along with the impedance of the basilar membrane at those frequencies. The basilar membrane impedance depends on

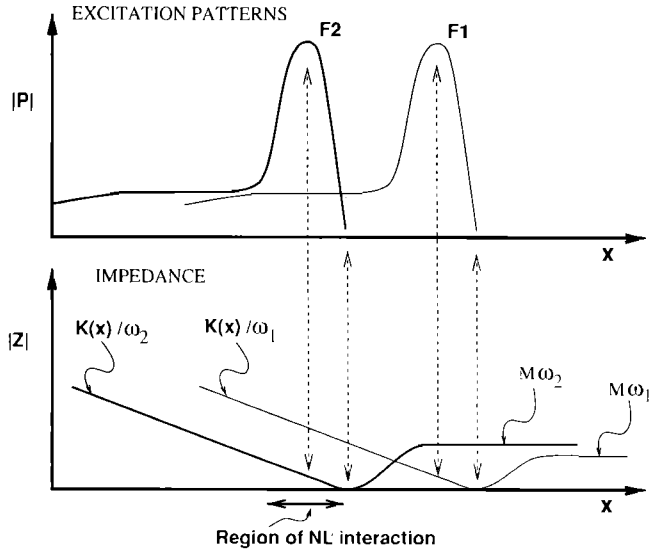

FIG. 11. We show here the relation between the basilar membrane impedance and neural excitation patterns for the two primary tones used to generate the DPs. At the place of generation, x_2, the impedance at radian frequency ω_1 ($\omega_1 = 2\pi f_1$) is stiffness dominated. For a nonlinear element to generate distortion products, it must have motion at both frequencies. Since almost all of the motion at the lower frequency f_1 is across the BM stiffness at the generator cite x_2, the nonlinear element must be the BM stiffness.

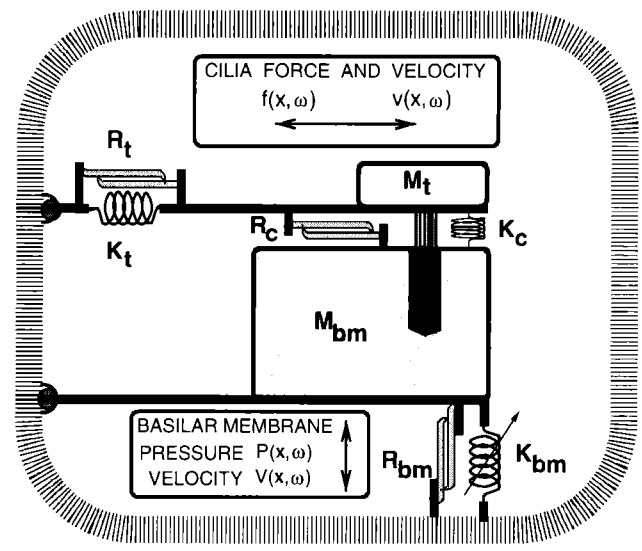

FIG. 12. In this figure we show a cross section of the organ of Corti, represented as a model of springs, masses and dash-pots (mechanical resistors). This model is a physical realization of two impedance model shown in Fig. 10.

position along the cochlea, as well as frequency. In the figure we show how the impedance varies along the basilar membrane at the two primary frequencies. At the f_2 place x_2, at frequency f_1, the impedance is dominated by the stiffness of the basilar membrane because the stiffness reactance is inversely proportional to the frequency. In physical terms, this means that most of the motion at f_1 is in the stiffness element, rather than in the resistive or mass elements. At frequency f_2 and place x_2, the impedance is still stiffness dominated, but to a lesser extent. From models we know that the high frequency cut-off slope corresponds to the resonant frequency of the basilar membrane impedance. Thus we have aligned these two points in the figure.

If a mechanical nonlinear element is to generate distortion products, it must move at both input frequencies. Since the only element at the f_2 place to move significantly at frequency f_1 is the stiffness, *the stiffness must be the nonlinear element.* We have shown this nonlinear motion as a Thévenin pressure source P_{dp} in Fig. 10.

B. The resonant TM model

A possible physical realization of the generic model of Fig. 10 is the physical model shown in Fig. 12 obtained by the introduction of an elastic element K_t in series with the tectorial membrane (TM) (Allen, 1980).

At low frequencies, below the resonant frequency of the TM, downward motion of the basilar membrane pulls the TM in phase with the reticular lamina (RL) (e.g., to the right). The hair cell cilia stand between the RL and the TM, defining the subtectorial space. The resulting shear between these two surfaces depends on the relative stiffness of the cilia K_c and the TM K_t. If K_c is 30 times stiffer than K_t, then the TM-RL shear will be 30 times smaller than the basilar membrane motion. As the frequency increases above the resonant frequency of the TM, the relative motion of the TM reverses. This means that it is moving to the left as the BM is pushed down. This change in phase means that the full motion of the BM must appear across the TM-RL surface.

One effect of the resonant TM is to isolate the cilia from low-frequency motions. It also would have the effect of reducing the low frequency Brownian motion of the cilia because it reduces the real part of the mechanical impedance seen by the cilia. This means that this structure is ideal from a noise analysis point of view. We show the stiffness of the BM as a nonlinear element by drawing an arrow through it. We assume that this stiffness decreases as the outer hair cells are depolarized. We leave the details of this discussion to a future paper (see also Allen, 1990; Allen and Neely, 1992).

V. DISCUSSION

We started by asking a question about the nonmonotonic behavior of the ear canal distortion products. We showed that a cochlear micromechanical filter, tuned to $f_d^*(x_2)$ [Eq. (1)] must be invoked to account for the independence of the maximum with distortion product order. We then argued that if the distortion products are filtered, there may be a corresponding filtering of the neural tuning curves. In fact such a relationship was found. We showed that the $f_d^*(f_2)$ was correlated to the tip-tail frequency of the frequency tuning curves and excitation patterns. We defined this frequency as $f_2(x_{CF})$, which defines a second cochlear map. We showed that one resonant impedance can filter both the ear canal distortion products and the cilia excitation in the observed way if it appears as a velocity shunt across the hair cells, leading to the generic

circuit shown in Fig. 10. Based on an impedance argument, we argued that the nonlinear element must be the basilar membrane stiffness, with the stiffness decreasing as the outer hair cells are depolarized.

The identification of $f_z(x)$, and its relation to both the minimum in the tuning mechanism and the maximum in the DP generation, quantitatively establishes tuned micromechanical processes. We have accounted for this correlation with a second shunt resonance $Z_t(f,x)$ within the organ of Corti, and summarized our observations with the diagram of Fig. 10 and the transfer functions defined in the previous section.

This model is further supported by other compelling evidence:

- Basilar membrane measurements do not show the tip-tail pattern commonly seen in high frequency neural tuning curve plots. No measured basilar membrane data has ever claimed to have tip-tail junctions that are as well defined as those of neural tuning curves at high frequencies.
- The neural population studies of Kim *et al.* found a 180-degree leading phase shift at x_z. Equation (13) in fact "predicts" this phase shift at the resonant frequency of Z_t, namely at f_z. For more discussion, see Fig. 4, of Allen, 1980, page 1663.
- Basilar membrane measurements do not show the 180-degree phase shift at x_z found by Kim *et al.* in neural population studies. No basilar membrane phase measurements have never shown this feature.
- Neural data shows that two-tone rate suppression occurs with sub-threshold suppressors (Fahey and Allen, 1985). Hall (1980) argued that this required a "second filter" to remove the response of the suppressor after it has suppressed the probe.
- The place where the motion of the cilia is shunted off by Z_t is also the place where the maximum forces appear across the cilia. This might explain why the maximum damage due to high level tones occurs at a point that is approximately 1/2 octave basal to the characteristic frequency, namely at x_z.
- The nonlinear component of the cochlear microphonic, the summating potential or SP, is known to change sign as the frequency is increased (Dallos, 1973). This might be explained by the 180 degree phase shift at $f_z(x)$.
- There are data that show that as f_1 approaches f_2 the psychophysical distortion products do not decrease for those f_1's where the ear canal distortion products are decreasing (Goldstein, 1967). This is consistent with the circuit of Fig. 10, as may be shown by calculating the transfer function v/P_{dp}. As the frequency of f_d is increased above the resonant frequency of Z_t, less current is shunted by that impedance, and more is passed to the cilia.

VI. CONCLUSION

The data and the analysis in this study show that a second cochlear map can be constructed that correlates neural tuning response data with ear canal distortion product data. A way to understand this correlation is depicted in Fig. 10 and a possible physical realization of Fig. 10 is shown in Fig. 12. If the models schematized in Fig. 10 and Fig. 12 are correct, then a second cochlear map should also be measureable in other animals that have both nonlinear mechanical basilar membrane responses and tectorial membranes.

ACKNOWLEDGMENTS

We would like to thank A. Brown, reviewer D. Greenwood, M.M. Sondhi, S. Puria, and P.S. Jeng for their generous help, and M.C. Liberman and B. Delgutte for access to the EPL neural tuning data. We would like to give special thanks to Steve Neely for discussions on the location of the nonlinear element, Sec. IV A.

Allen, J.B. (1980). "Cochlear micromechanics—A physical model of transduction," J. Acoust. Soc. Am. 68, 1660–1670.

Allen, J.B. (1990). "Modeling the noise damaged ear," in *The Mechanics and Biophysics of Hearing*, edited by P. Dallos, C.D. Geisler, J.W. Matthews, M.A. Ruggero, and C.R. Steele (Springer-Verlag, New York), pp. 324–332.

Allen, J.B., and Neely, S.T. (1992). "Cochlear micromechanics," Phys. Today 45, 40–47.

Brown, A.M., and Gaskill, S.A. (1990). "Can basilar membrane tuning be inferred from distortion measurement?," in *The Mechanics and Biophysics of Hearing*, edited by P. Dallos, C.D. Geisler, J.W. Matthews, M.A. Ruggero, and C.R. Steele (Springer-Verlag, New York), pp. 164–169.

Brown, A.M., and Gaskill, S.A., and Williams, D.M. (1992). "Mechanical filtering of sound in the inner ear," Proc. R. Soc. London Ser. B 250, 29–34.

Dallos, P. (1973). *The Auditory Periphery* (Academic, New York).

Fahey, P.F., and Allen, J.B. (1985). "Nonlinear phenomena as observed in the ear canal and at the auditory nerve," J. Acoust. Soc. Am. 77, 599–612.

Fahey, P.F., and Allen, J.B. (1986). "Characterization of cubic intermodulation distortion products in the cat external auditory meatus," in *Peripheral Auditory Mechanisms*, edited by J.B. Allen, J.L. Hall, A. Hubbard, S.T. Neely, and A. Tubis (Springer-Verlag, New York), pp. 314–321.

Fahey, P.F., and Allen, J.B. (1988). "Power law features of acoustic distortion product emissions," in *Basic Issues in Hearing*, edited by H. Duifhuis, J.W. Horst, and H.P. Wit (Academic, London), pp. 124–131.

Greenwood, D.D. (1990). "A cochlear frequency-position function for several species—29 years later," J. Acoust. Soc. Am. 87, 2592–2605.

Goldstein, J.L. (1967). "Auditory nonlinearity," J. Acoust. Soc. Am. 41, 676–689.

Hall, J.L. (1974). "Two-tone distortion products in a nonlinear model of the basilar membrane," J. Acoust. Soc. Am. 56, 1818–1828.

Hall, J.L. (1980). "Cochlear models: two-tone suppression and the second filter," J. Acoust. Soc. Am. 67, 1722–1728.

Kim, D.O., Siegel, J.H., and Molnar, C.E. (1979). "Cochlear nonlinear phenomena in two-tone responses," Scand. Audiol. Suppl. 9, 63–82.

Kim, D.O., Molnar, C.E., and Matthews, J.W. (1980). "Cochlear mechanics: Nonlinear behavior in two-tone responses as reflected cochlear-nerve-fiber responses and in ear-canal sound pressure," J. Acoust. Soc. Am. 67, 1704–1721.

Liberman, M.C. (1982). "The cochlear frequency map for the cat: Labeling auditory-nerve fibers of known characteristic frequency," J. Acoust. Soc. Am. 72, 1441–1449.

Matthews, J.W., and Molnar, C.E. (1986). "Modeling of intracochlear and ear canal distortion product $2f_1-f_2$," in *Peripheral Auditory Mechanisms*, edited by J.B. Allen, J.L. Hall, A. Hubbard, S.T. Neely, and A. Tubis (Springer-Verlag, New York), pp. 258–265.

Whitehead, M.L., Lonsbury-Martin, B., and Martin, G.K. (1992). "Evidence for two discrete sources of $2f_1-f_2$ distortion-product otoacoustic emission in rabbit: I. Differential dependence on stimulus parameters," J. Acoust. Soc. Am. 91, 1587–1607.